higher fo_2 conditions in the high-Ti suite, compared to the low-Ti volcanics; between QFM and higher than QFM + 1.

The mantle source of the low-Ti volcanics was LREE enriched (i.e. E-MORB and/or higher subduction flux[20]) compared to the high-Ti volcanics. Higher proportions of garnet in the mantle residue of the low-Ti volcanics retained Ti, HREE and Sc compared to the high-Ti volcanics. Therefore, the subtle major and minor element differences between the arc-related high-Ti and low-Ti volcanics (Figures 1–3) are neither related to elemental mobility, nor can they be explained by clinopyroxene and plagioclase fractionation[21], but are due to different degrees of partial melting of a heterogeneous mantle source (with respect to garnet) under different P_{H_2O}, fo_2 and subduction fluxing conditions.

The enriched MORB source of the low-Ti volcanics implies early stages of back-arc spreading, as in the Izu-Marianas arc or interarc rifting[20] and provides a simple explanation for the paradoxial presence of interlayered sedimentary formations of the Khairagarh Group[7]. Similarly, the presence of only tholeiitic lavas in the Khairagarh volcanics indicates the subduction of a relatively young and thin (< 20 km) oceanic plate with relatively high (> 7 cm/yr) convergence rates[22].

1. Walker, J. A., Carr, M. J., Feigenson, M. D., Kalamarides, R. I., *J. Petrol.*, 1990, **31**, 1141–1164.
2. Eggins, S. M., *Contrib. Mineral. Petrol.*, 1993, **114**, 79–100.
3. Yogodzinski, G. M., Rabenstone, J. L., Kay, S. M. and Kay, R. W., *J. Geophys. Res.*, 1993, **98**, 11807–11834.
4. Baker, M. B., Grove, T. L. and Richard, P., *Contrib. Mineral. Petrol.*, 1994, **118**, 111–129.
5. Raza, M. J., Alvi, S. H. and Khan, M. S., *J. Geol. Soc. India*, 1993, **41**, 455–469.
6. Sun, S. S. and Nesbitt, R. W., *Geology*, 1978, **6**, 689–693.
7. Neogi, S., Miura, H. and Hariya, Y., *Precambr. Res.*, 1996, **76**, 77–91.
8. Khare, S. K., Asthana, D., Dash, M. R. and Pophare, A. M., *J. Geol. Soc. India*, 1996, communicated.
9. Deshmukh, G. G., Mohabey, N. K. and Deshpande, M. S., *Geol. Surv. India, Spl. Publ. no. 28*, 260–286.
10. Sarkar, S. N., *Indian J. Earth Sci.*, 1994, **21**, 117–126.
11. Govil, P. K., *J. Geol. Soc. India*, 1985, **26**, 38–42.
12. Balaram, V., *Curr. Sci.*, 1985, **69**, 640–649.
13. Davies, J. F. and Grant, R. W. E., *Can. J. Earth Sci.*, 1979, **16**, 305–311.
14. Feigenson, M. D. and Carr, M. I., *Contrib. Mineral. Petrol.*, 1993, **113**, 226–235.
15. Carr, M. J., Feigenson, M. D. and Bennett, E. A., *Contrib. Mineral. Petrol.*, 1990, **105**, 369–380.
16. Thirlwall, M. F., Smith, T. E., Graham, A. M. and Theodorou, N., *J. Petrol.*, 1994, **35**, 819–838.
17. Gaetani, G. A., Grove, T. L. and Bryan, W. B., *Nature*, 1993, **365**, 332–334.
18. Gaetani, G. A., Gove, T. L. and Bryan, W. B., Proc. Ocean Drilling Project, 1994, LEG 135, pp. 557–563.
19. Pearce, J. A. and Parkinson, I. J., in *Magmatic and Plate Tectonics* (eds Pricard, H. M., Alabaster, T., Harris, N. B. W. and Neary, C. R.), *Geol. Soc. Spl. Publ. no. 76*, 1993, pp. 373–403.
20. Pearce, J. A. and Peate, D. W., *Annu. Rev. Earth Planet. Sci.*, 1995, **23**, 251–285.
21. Jahn, B. M., *Early Precambrian Basic Magmatism*, Chapman and Hall, New York, 1990, pp. 294–317.
22. Gill, J. B., *Orogenic Andesites and Plate Tectonics*, Springer-Verlag, New York, 1981, p. 390.
23. Krishnamurthy, P., personal communication, 1996.

ACKNOWLEDGEMENTS. We thank CSIR for funding the study and the Geochemistry Section of NGRI for carrying out the analysis. This work forms part of the Ph D work of M. R. Dash.

Received 17 June 1996; accepted 15 July 1996

Unusual aspects of pressure-induced phase transitions in $CuGeO_3$

A. Jayaraman, S. K. Sharma, S. Y. Wang and S-W. Cheong*

University of Hawaii, Hawaii Institute of Geophysics and Planetology, Honolulu, HI 96822, USA
*Lucent Technologies, Bell Labs Innovations, Murray Hill, NJ 07974, USA

High pressure Raman and optical studies on the spin-Peierls compound $CuGeO_3$ have revealed three novel pressure-induced phase transitions in the 7–8 GPa range. One of these occurring only under hydrostatic conditions, is believed to be a ferroelastic–ferroelectric phase. The other two high pressure phases are brilliant blue and green, respectively. Of these, the blue-phase is quenchable, while the green-phase reverts to the blue. From crystal chemistry, Raman spectral features and metastability considerations, it is suggested that the blue and the green phases have the pyroxene type chain structure similar to enstatite polymorphs, and non-hydrostatic pressure is essential for the formation of pyroxene type chain structures.

COPPER metagermanate ($CuGeO_3$) is a very interesting material, for it is the first inorganic system that exhibits the so-called spin-Peierls transition[1], when cooled below 14 K at ambient pressure. It is a very soft layer-type light blue material (like mica), crystallizing in the orthorhombic space[2] group Pbmm (C^5_{2h}). The backbone of the structure consists of chains (parallel to the *c*-axis of the crystal) of corner shared GeO_4 tetrahedra linked by edge-sharing CuO_6 octahedral chain co-parallel to the GeO_4 chain[2], as shown in Figure 1 on the left. The structure is related to the pyroxene family minerals, viz. enstatite, but differs from it in having a unique arrangement of GeO_4 tetrahedra called 'einer' chain, stabilized

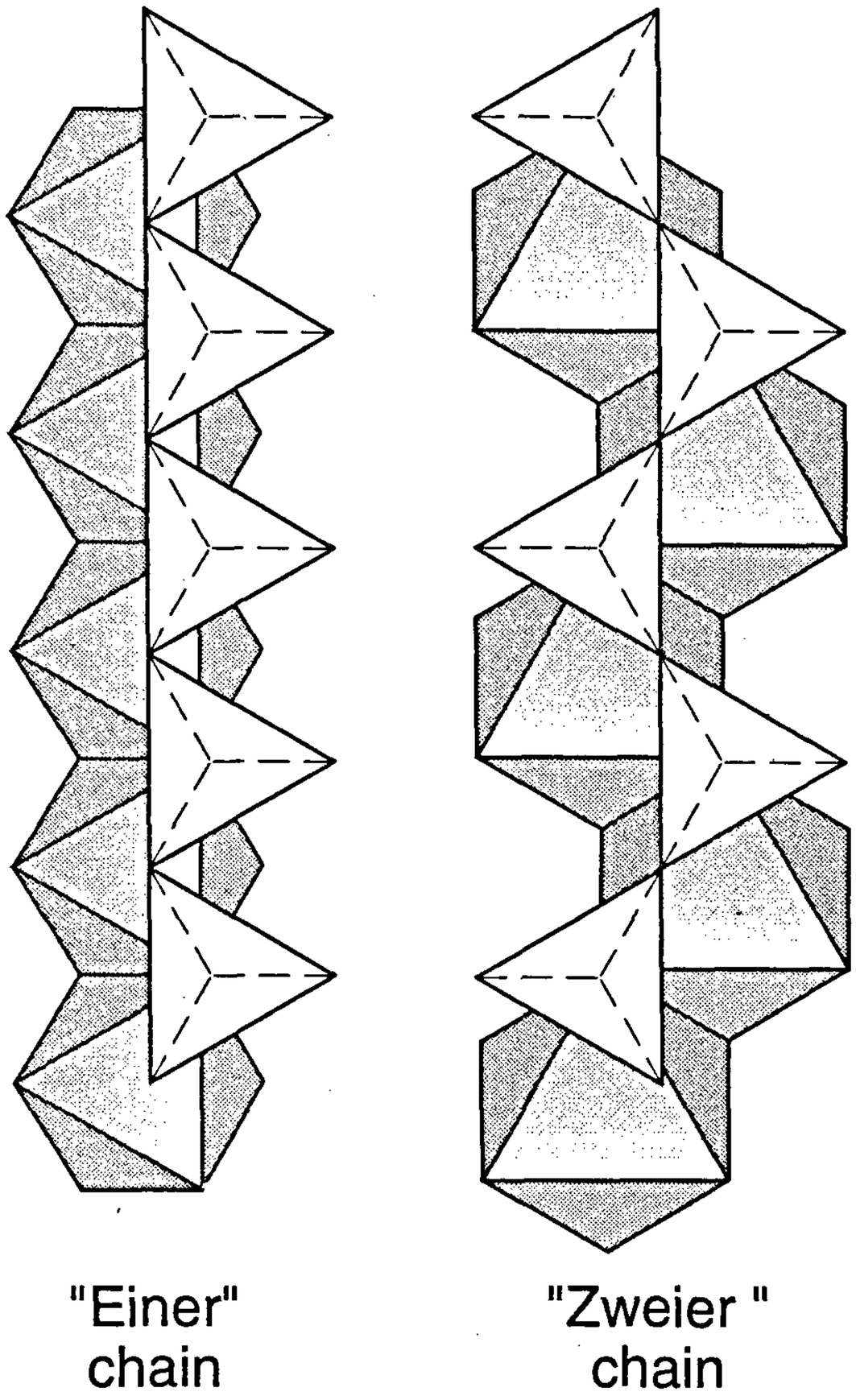

Figure 1. The tetrahedral GeO_4 corner sharing extended 'einer' chain with the CuO_6 edge sharing octahedral chain, the backbone of the $CuGeO_3$ structure. On the right is a pyroxene type extended 'zweier' chain. The chains run parallel to the *c*-axis of the crystal. Note that all the tetrahedra are on the same side in 'einer' chain whereas in the pyroxene type chain they alternate between the two sides of the chain.

by the tendency of the copper to have Jahn–Teller distorted CuO_6 octahedra. In the 'einer' chain, all of the tetrahedra units lie on the same side of the chain, while in a pyroxene chain they lie on either side (see Figure 1 right side).

From the point of view of high pressure behaviour also, $CuGeO_3$ is turning out to be very interesting. Our previous high pressure Raman and optical studies on the system[3] have revealed the occurrence of a rather unusual type of reversible phase transition near 7 GPa, when 4:1 methanol/ethanol mixture was used. Further extensive studies of the high pressure behaviour of $CuGeO_3$ carried out recently using Raman spectroscopy and optical microscopy, with a variety of pressure media and with single crystal and powder samples have yielded a wealth of details. The high pressure behaviour of $CuGeO_3$ is spectacular and quite complex. We will illustrate some novel aspects of the pressure-induced transitions and discuss them briefly here. A detailed account will be published elsewhere.

Three distinct high pressure phases are encountered in the 7–9 GPa region, when the normal orthorhombic (Phase I) Pbmm (D^5_{2h}) phase of $CuGeO_3$ (Pmma in the standard notation) is compressed. Surprisingly, the type of phase obtained depends on the hydrostaticity of the pressure medium near 8 GPa. This is shown diagramatically in Figure 2. Thus when methanol/ethanol mixture, pure methanol or helium is used, the sample abruptly contracts by about 15% in the *b*-direction of the crystal, near 7 GPa. The resultant high pressure phase which we label as Phase II is pale green and has a different Raman spectrum. On pressure release, the reverse transition takes place near 5.6 GPa. This phase (I to II) transition was first observed in methanol/ethanol mixture earlier, and its amorphization above 15 GPa was documented in the earlier publication by Jayaraman *et al.*[3] In the present study, we have observed this very same transition with helium which is a perfect hydrostatic medium up to 11.8 GPa at room temperature[4], and also in pure methanol which freezes just a little above 7 GPa. The photomicrographs reproduced in Figure 3 show a single crystal sample of $CuGeO_3$ at different pressures in helium gas as pressure medium in the diamond cell. Figure 3*c* is the high pressure phase (Phase II). The contraction in the *b*-axis direction is striking. In Figure 4, the Raman spectrum of $CuGeO_3$ at 1 bar and at 7.9 GPa in helium is presented.

When argon is used as a pressure medium, the original phase starts to turn blue (designated Phase III) near 7.5 GPa. While this transition is progressing, another phase transition intrudes and the colour of the sample changes to green (designated Phase IV). This transition starts as green stripes traversing the crystal, and then covers the entire sample with increasing pressure. The change in the colour is accompanied by changes in the Raman spectral features. The green phase is stable up to 15 GPa, as judged from its Raman spectral features. When pressure is released, the green-phase transforms to the blue phase near 5 GPa and the latter can be quenched to ambient pressure. The quenched blue phase can be reversed to the original orthorhombic phase, only by heating to 600°C. The blue phase on repressurization transforms to the green phase near 8 GPa and the transformation can be recycled back and forth, irrespective of the pressure medium used. Further, there are no striking changes in the sample dimension accompanying the phase III $\rightleftharpoons$ IV transitions, and the singe crystal nature is preserved. In Figure 5, colour photomicrographs of Phase I at two pressures and Phase III and IV at 4 GPa (pressure release cycle) and 11 GPa respectively are

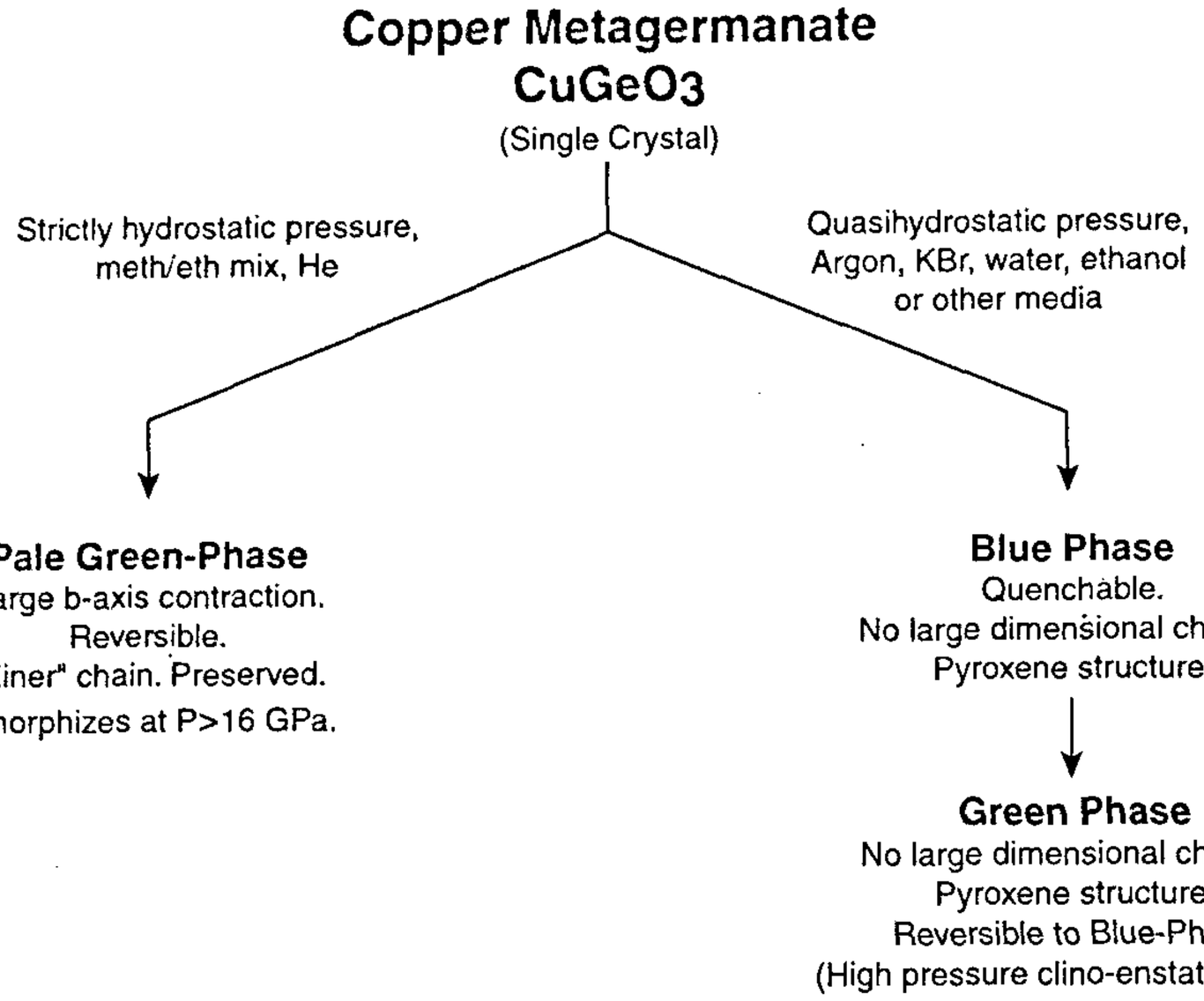

Figure 2. Diagrammatic representation showing the forking of the pressure-induced phase transitions in $CuGeO_3$, depending on the nature of stress.

presented. The pressure medium was argon. The Raman spectra of the green phase (IV) recorded near 5.6 GPa, and of the blue phase (III) near 4 GPa (both on the pressure release cycle) are shown in Figure 6.

With all other pressure media, the results obtained are similar to those described in the case of argon since they freeze before 7 GPa. Argon freezes at 1.2 GPa at room temperature. Potassium bromide (KBr) is a soft solid and therefore, behaves as a quasihydrostatic medium.

The results presented raise two main questions: (1) what are the structures of the three high pressure phases and (2) why does the hydrostaticity of the pressure medium have such a strong influence on the nature of the phase transition? Obviously a definite answer to the first question must come from high pressure X-ray diffraction studies on the high pressure phases, preferably single crystal diffraction. An earlier energy dispersive X-ray diffraction study[5] on $CuGeO_3$ powder up to 20 GPa reported a phase transition near 7 GPa. For the high pressure phase, a monoclinic cell of $P2_1/m$ symmetry has been proposed. Quite recently, Haines and Adams[6] have commented that the phase transition reported by us on single crystal $CuGeO_3$ (ref. 3) must be the same as the orthorhombic to the monoclinic phase mentioned, and not due to intercalation, as we had suggested. Our experience with $CuGeO_3$ powder is that the Phase I to II transition does not occur unless pressurization is carried out in a hydrostatic medium. From our new findings presented in this paper, it appears to us that the phase transition reported in the X-ray study is most likely to be from the normal orthorhombic to the green phase.

We will now discuss some possible structures for the blue and the green phases of $CuGeO_3$, in the light of the known high pressure crystal chemistry of silicate pyroxenes[7,8], and the structural features of other metagermanates[9]. In silicate pyroxenes, the SiO_4 tetrahedra form infinite chains by corner sharing along the *c*-axis of the crystal, and the chains are linked by cation polyhedra to form the structure. The tetrahedra lie on either side of the chain (see Figure 1) connected by bridging oxygens and is called a 'zweier' chain, because the periodicity along the *c*-axis is twice the distance of the bridging oxygens. The most important difference between the pyroxene and $CuGeO_3$ is the so-called 'einer' chain feature, which is unique to this compound[2]. The stability of this chain is believed to be very low because of the strong repulsion of the highly-charged Ge^{4+} ions[10]. It is the energy gain resulting from the Jahn–Teller distortion of Cu that stabilizes the structure. The pyroxene type 'zweier' chain appears more natural for $CuGeO_3$. In fact $MgGeO_3$ has the usual pyroxene type GeO_4 chain and is known to crystallize in the ortho-enstatite (Pbca) and clino-enstatite ($C2/c$) structure[9]. Thus, we can expect $CuGeO_3$ to transform from the 'einer' chain type to the pyroxene type of structure at high pressure.

For the blue phase, we suggest the ortho (Pbca) or the low clino-enstatite structure ($C2/c$), based on crystal chemistry, Raman spectral feature and quenchability. Thus, (i) the magnesium compound $MgGeO_3$ under

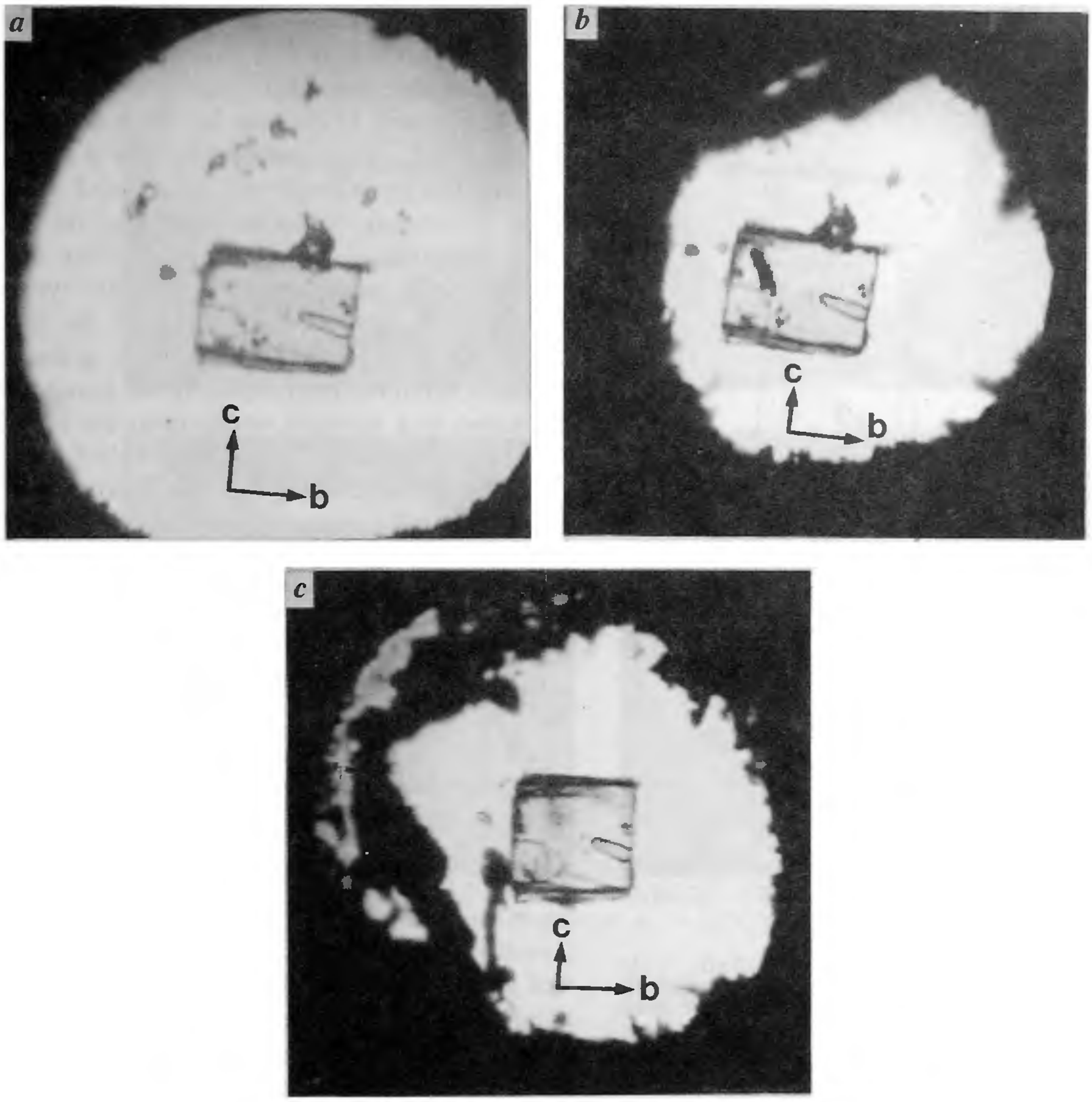

Figure 3 *a–c*. Photomicrographs of $CuGeO_3$ single crystal in the diamond cell at three different pressures, with helium as pressure medium (*a*) 0.5 GPa (*b*) 5.2 GPa and (*c*) 8 GPa. The *b* and *c*-axis of the original orthorhombic crystal is marked. Note the large contraction in the *b*-direction in (*c*). Helium freezes at 11.8 GPa at room temperature and is a gas until then.

ambient conditions crystallizes in these structures[9], (ii) the observed splitting of the high frequency Raman peak (see Figure 5) representing the symmetric stretch is in accord with the splitting of this mode in both the low-clino and ortho-enstatite[11], (iii) finally, the quenchability shows that the pyroxene chain is established in the blue-phase: A change from orthorhombic (Pbmm) $CuGeO_3$ to pyroxene-type structure must involve a 180° flipping of alternate GeO_4 tetrahedra, to convert the 'einer' chain to 'zweier' type chain and this transition involves breaking of bonds and flipping of the CuO_6 octahedra as well. Once this happens under high pressure, the reverse transition would be kinetically impeded. The observed quenchability of the blue phase and its reversion, only when heated to 600°C is consistent with the above expectation.

Our optical observations in polarized light indicate that the single crystal nature is preserved in the blue phase. Hence, it should be possible to carry out single crystal X-ray diffraction on quenched blue phase and the structural prediction verified. In this phase, the spin-Peierls transition should be absent because of the change in the Cu^{2+} array due to conversion to the 'zweier' type chain.

Once the essential ingredient for the pyroxene structure is established, namely the 'zweier' chain, the behavior of $MgSiO_3$ under pressure could be used as a guide. It has been shown that both clino-enstatite ($MgSiO_3$)[12] and ferrosilite ($FeSiO_3$)[13] transform under high pressure to a high pressure *C2/c* phase near 7 GPa and 1.75 GPa, respectively. This phase is denser by about 3% compared to the original phase[13]. The transitions in both

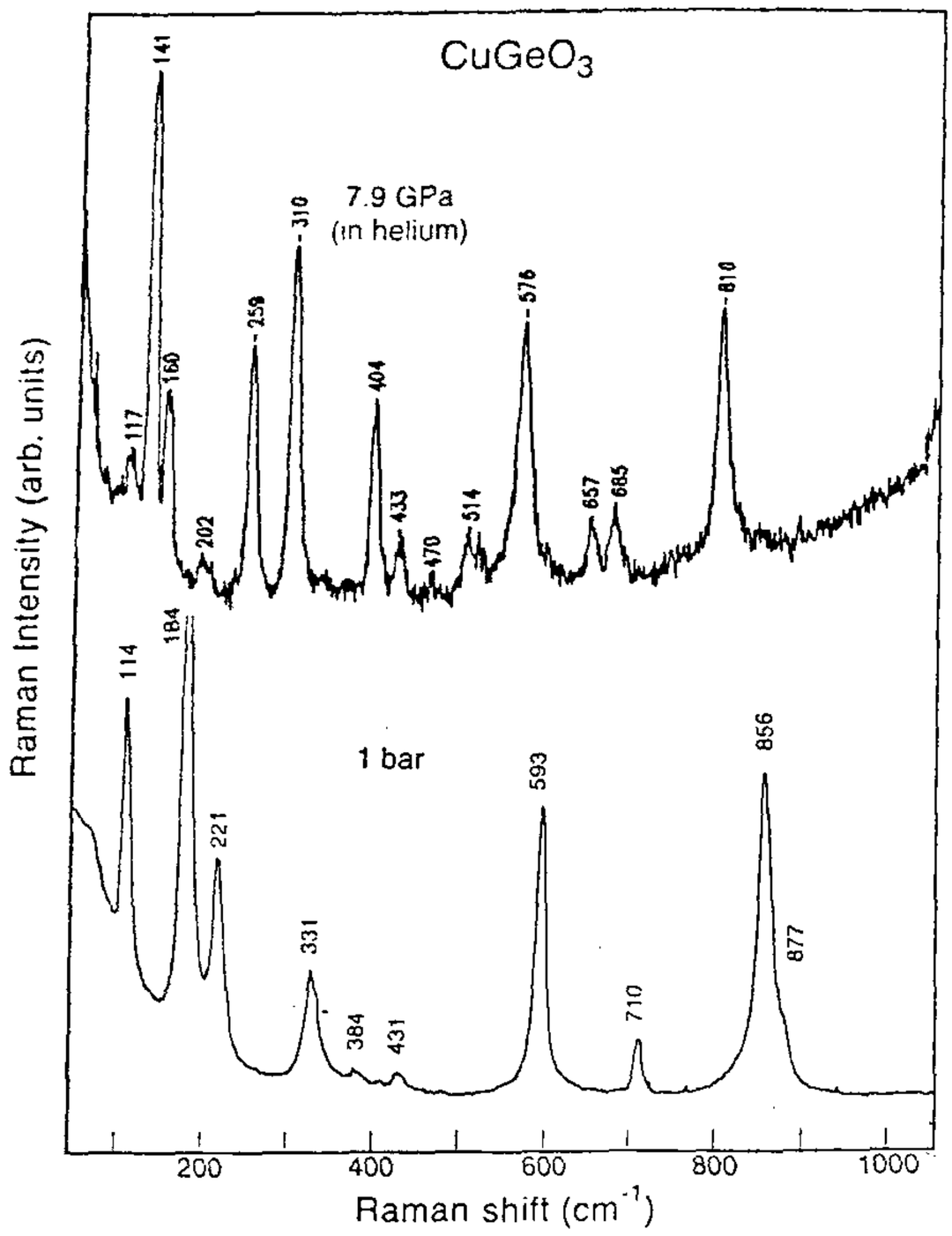

Figure 4. Raman spectrum of single crystal sample of orthorhombic $CuGeO_3$ at ambient pressure (bottom) and 7.9 GPa, after the phase transition to Phase II. Pressure medium was helium gas. The spectrum is identical to that obtained with methanol/ethanol mixture, as medium.

$MgSiO_3$ and $FeSiO_3$ are reversible. The low to high-pressure clino-enstatite transition involves a change from two symmetrically-distinct tetrahedral chains rotated in opposite directions to one symmetrically-distinct tetrahedral chain. We suggest that a similar phase transition occurs in the green phase of $CuGeO_3$. Its reversibility and the Raman spectral feature support this interpretation.

The pale green phase–phase II transition occurs only when the pressure medium is *strictly hydrostatic* and not otherwise, and is a very unusual behaviour. For this phase transition, intercalation by the pressure medium (alcohol) was suggested[3]. However, the occurrence of the very same transition with helium gas also, throws some doubt on the intercalation idea. The presence of a single strong Raman peak in the υ_s (Ge–O–Ge) and υ_s ($Ge–O^-$) mode region (see Figure 1) is a strong indication that the 'einer' chain feature is preserved in this phase.

All the evidence we have accumulated so far point to the fact that this Phase I to II transition is abrupt and cannot involve any bond breaking. A sliding or partial rotation of the chain must occur in the structure, to cause the crystal to contract abruptly in the *b*-axis direction. If the crystal is constrained by a solid pressure medium, this contraction will be impeded and the transition suppressed. When this happens, the competing phase transition to the pyroxene structure takes over, and the 'einer' chain turns into pyroxene-type 'zweier' chain, to minimize the free energy of the compressed system, triggering the blue and then the green phase sequence. Therefore, the freedom for the *b*-axis to contract or expand is a stringent requirement for I to II phase transition to occur. This would explain the extreme sensitivity of the transition to the hydrostaticity of the medium. These aspects suggest that phase II might be a strongly-coupled ferroelastic system. Usually a ferroelastic transition is coupled to a ferroelectric transition also. One of the sure indications for the latter would be the presence of ferroelectric domains. However, we do not observe any domains in the high pressure phase II when examined in crossed polarization under the microscope. But we believe that the observed jumping of the crystal inside the diamond cell at the transition when helium is used as a pressure medium is significant, and may be connected with the development of electric charge in the crystal due to the sudden compression in the *b*-axis direction of the crystal. That a ferroelectric crystal when suddenly compressed can get charged is well known. Therefore, it may be that this high pressure phase II of $CuGeO_3$ is ferroelectric–ferroelastic. Such a coupled situation is known, as is exemplified in the β'-phase of $Tb_2(MoO_4)_3$ (ref. 14).

The high pressure behaviour of $CuGeO_3$ has many interesting facets. The elucidation of the structural features of the high pressure phases by single crystal X-ray diffractions is an inviting challenge to the crystallographer. Once the symmetry and space groups are determined, the interpretation of the vibrational spectra could lead to further insights into the high pressure behaviour. The anomalous *b*-axis compression carries the key to understand pressure-induced instabilities, just as it is significantly connected to the spin-Peierls instability at low temperatures. The large *b*-axis contraction at the I to II transition and the extreme sensitivity of the latter to the nature of applied stress suggests a strongly-coupled ferroelastic phase for phase II, with the possibility of ferroelectric behaviour in addition. Application of pressure is a route to prepare a new polymorph of $CuGeO_3$, namely, the blue phase at ambient pressure. The properties of this would be of interest. The colours of the phases are rooted in the electronic structure of Cu^{2+}, a $3d^9$ Jahn-Teller ion. A deeper understanding of the absorption features could connect, Jahn-Teller distortion, structure and absorption. Finally, the possibility of

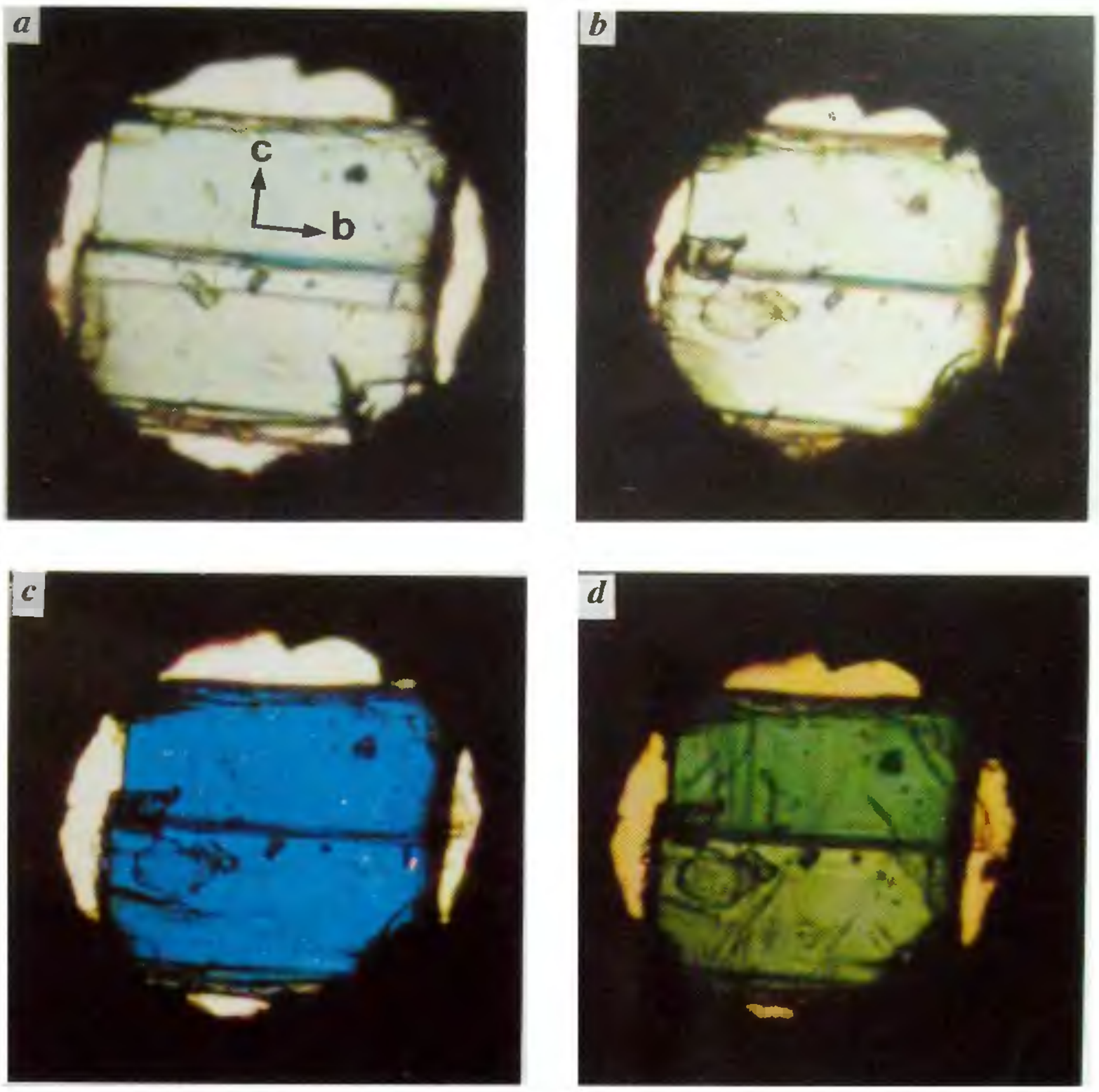

Figure 5. Colour photomicrographs of single crystal $CuGeO_3$ at four different pressures. Pressure medium argon (*a*) 1 GPa (*b*) 5 GPa (*c*) 4 GPa and (*d*) 11 GPa. (*b*) and (*c*) taken on the pressure release cycle. The *b* and *c*-axis of the original orthorhombic Pbmm phase marked.

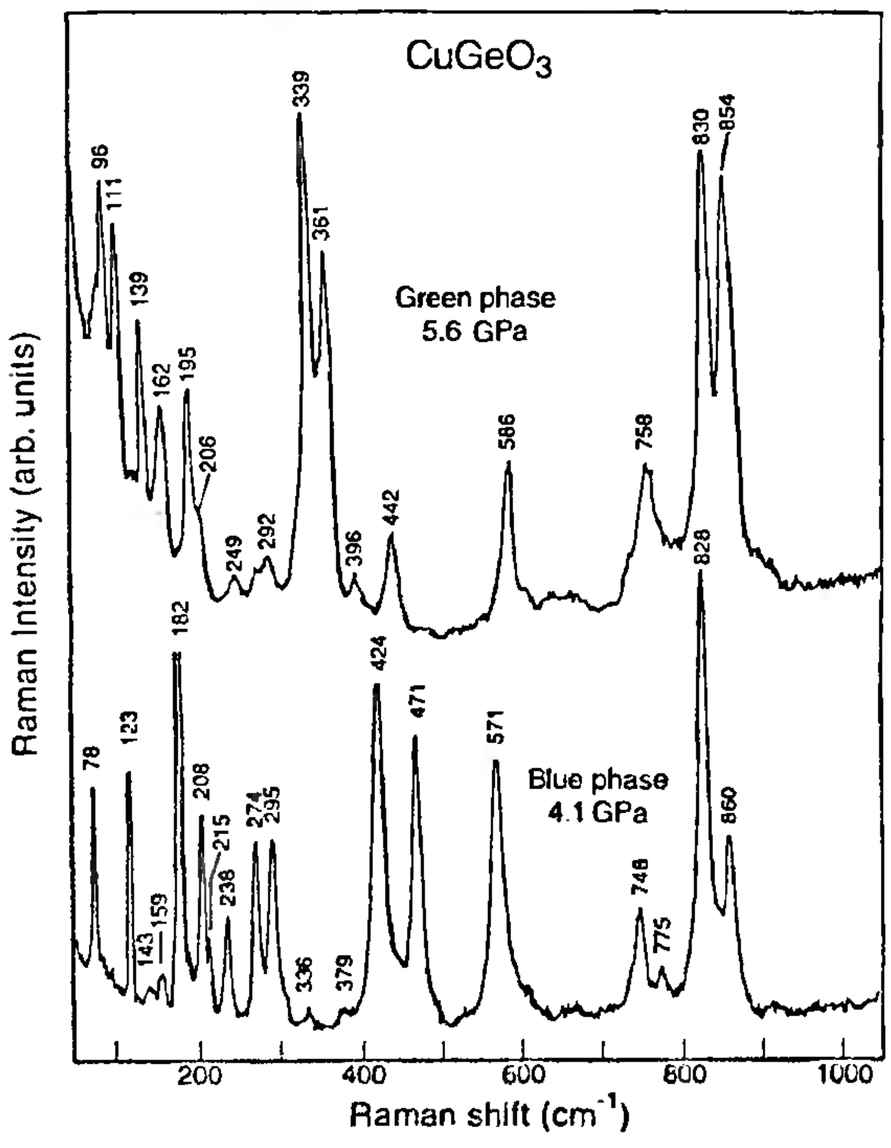

Figure 6. The Raman spectrum of $CuGeO_3$ single crystal sample in the blue-phase at 4.1 GPa, green-phase at 5.6 GPa, obtained on the pressure release cycle with 514.5 nm excitation. Note the splitting of the high frequency peaks (symmetric stretch).

phase transitions to garnet, ilmenite and perovskite structure exists, in analogy with the behaviour of other germanates and silicates.

1. Hase, M., Terasaki, I. and Uchinokura, K., *Phys. Rev. Lett.*, 1993, **70**, 3651–3654.
2. Völlenkie, H., Wittmann, A. and Nowotny, H., *Monatch. Chem.*, 1967, **98**, 1352–1357.
3. Jayaraman, A., Wang, S. Y., Ming, L C. and Cheong, S.-W., *Phys. Rev. Lett.*, 1995, **75**, 2356–2359.
4. Bell, P. M. and Mao, H. K., *Carnegie Institute of Washington, Year Book*, 1979, **78**, 404–406; Hazen, R. M., Mao, H. K., Finger, L. W. and Bell, P. M., *Carnegie Institute of Washington, Year Book*, 1980, **79**, 348–351; Mammone, J. F., Sharma, S. K. and Nicol, M., *J. Phys. Chem.*, 1980, **84**, 3130–3134.
5. Adams, D. M., Haines, J. and Leonard, S., *J. Phys. Condens. Matter*, 1991, **3**, 5183–5190.
6. Haines, J. and Adams, D. M., *Phys. Rev. Lett.*, 1996, **77**, 204–205.
7. Liebau, F., *Structural Chemistry of Silicates*, Springer-Verlag, Berlin, 1985; A. N. Lazarev, *Vibrational Spectra and Structure of Silicates*, Consultants Bureau, New York, 1972, p. 302.
8. Cameron, M. and Papike, J. J., in *Reviews in Mineralogy* (ed. Prewitt, C. T.), Miner. Soc. America, Washington, D.C., 1980, vol. 7, pp. 1–92.
9. Ozima, M. and Akimoto, S., *Am. Miner.*, 1983, **68**, 1199–1205; Ross, N. L. and Navrotsky, A., *Am. Miner.*, 1988, **73**, 1355–1365.

10. Behruzi, M., Breuer, K. H. and Eysel, W., *Z. Kristallogr.*, 1986, **176**, 205–217; Breuer, K. H., Eysel, W. and Behruzi, M., *Z. Kristallogr.*, 1986, **176**, 219–232.
11. Sharma, S. K., *Vibrational Spectra and Structure*, 1989, **B17**, 513.
12. Angel, R. J., Chopelas, A. and Ross, N. L., *Nature*, 1992, **358**, 322–324.
13. Hugh-Jones, D. A., Woodland, A. B. and Angel, R. J., *Am. Miner.*, 1994, **79**, 1032–1041.
14. Brixner, L. H., Barkley, J. R. and Jeitschko, W., in *Handbook on the Physics and Chemistry of Rare Earths* (eds Gschneidner, Jr. K. A. and Eyrng, L.), North Holland Publishing Co., Amsterdam, 1979, pp. 609–654.

ACKNOWLEDGMENTS. We thank Dr L. C. Ming and Dr A. S. Bhalla for helpful discussions and S. R. Shieh for valuable assistance. This work was supported by NSF grant DMR-94-02443. SOEST contribution no. 4122.

Received 25 June 1996; accepted 10 July 1996

Synthesis and anticancer activity of new derivatives of podophyllotoxin

Wang Yan-guang, Pan Jian-lin and Chen Yao-Zu*

Department of Chemistry, Zhejiang University, Hangzhou 310 027, P. R. China

A series of analogues of etoposide (VP-16,1), the C-4 alkylamino-substituted 4'-dimethyl-epipodophyllotoxins (4a-g), have been synthesized and studied for their activity to inhibit L1210 and KB cells *in vitro*. Compounds 4a, 4b, 4c and 4f are as potent or more potent than VP-16 in their inhibition of both L1210 and KB cells.

THE clinical efficacy and intriguing mechanism of podophyllotoxin-derived glucoside, etoposide (VP-16, 1), has greatly stimulated interest in the synthesis of new active analogues of podophyllotoxin[1–6]. The approach to modify 1 based on replacement of the glucose moiety with an amino sugar has led to some highly active analogues[3], suggesting that β-anomeric configuration was indispensable for the antitumour activity and that the amino substituent of the sugar moiety was important for increasing the activity. Changes in the 4β-glycosyl group are also of interest for simplified structure which might retain the activity of 1 and its amino glucoside analogues, and be accessible to practical industrialization. In the previous papers[4,7,8], we reported the synthesis of an amino nitroxyl spin-labeled analogue of 1, GP-7(2), which exhibited superior pharmacological properties to 1. A series of 4β-alkylamino and arylamino derivatives of 4'-demethylepipodophyllotoxin, such as 3a–c, have also demonstrated by the strong antitumour activity that considerable simplification in the sugar structure might be permitted so long as the amino group was retained[5,6,9]. These findings prompted us to change the C-4 glucose moiety in VP-16 to a configurationally similar amino-acid ester, and to synthesize seven new derivatives of podophyllotoxin (4a–g).

4β alkylamino derivatives of 4'-demethylepipodophyllotoxin (4a–g) were synthesized by direct nucleophilic substitution (SN1) of appropriate L-amino-acid ester (7a–g) with 4β-bromo-4'-demethyl-4-deoxypodophyllotoxin (6) resulting from podophyllotoxin (5). The bulky C-1α pentant aromatic ring dictates the substitution to be stereoselective in yielding the C-4β alkylamino isomers as the major products. In some cases, the C-4α isomers were also observed. The assignment of the configuration at C-4 for compounds 4a–g was based on the difference of $J_{3,4}$ coupling constants. The C-4β-substituted compounds 4a–g have a $J_{3,4} \approx 4.0$ Hz as seen in 1 and 3 (refs. 5, 6), due to a *cis* relationship between H-3 and H-4. The C-4α substituted derivatives, however, have a $J_{3,4} \geq 10.0$ Hz as H-3 is *trans* to H-4 (ref. 6).

We have tested the inhibitory activities of compounds 4a–g against leukaemia L1210 and KB cells *in vitro*. ID_{50} values of compounds 1 and 4a–g are 0.40, 0.28, 0.42, 0.38, 0.70, 1.60, 0.42 and 1.25 μM for L1210 cells, and 0.22, 0.20, 0.10, 0.18, 0.56, 0.84, 0.28 and 1.00 μM for KB cells, respectively. Therefore, compounds 4a, 4b, 4c and 4f are as potent or more potent than VP-16 in their inhibition of both L1210 and KB cells. These results demonstrate the possibility of considerable simplification in the sugar structure of 1 and suggest further elaboration of the 4β-amino substituent to optimize the structure of this class of anticancer compounds. Further study for anticancer activity of synthesized compounds is in progress.

All melting points were taken on Yanaco melting point apparatus and uncorrected. IR spectra were obtained on a nicolet-5DX spectrophotometer, and ^{1}HNMR spectra were obtained by using either a Bruker AM-400 or JMS-FX-90Q NMR spectrometer. All chemical shifts are reported in ppm from TMS. Elemental analysis were taken on a YANACO-CHN-CODER MT-3 instrument. MS analysis were determined on a VG-7070E-HF instrument at 70 eV.

A solution containing 4β-bromo-4'-demethyl-4-deoxypodophyllotoxin (6) (ref. 1) (1.5 mmol), anhydrous barium carbonate (2.0 mmol), and the appropriate L-amino-acid ester (7a-g) (2.0 mmol) in 20 ml of dry 1,2-dichloroethane under nitrogen was stirred overnight at room temperature. The reaction mixture was filtered, diluted with ethyl acetate, washed with water, dried, and purified via column chromatography (50 g of silica gel with dichloromethane-acetone 8:1 as eluant). Yields ranged from 18 to 47%.